The Journal of Systems and Software 85 (2012) 2459–2469

Contents lists available at SciVerse ScienceDirect

The Journal of Systems and Software

journal homepage: www.elsevier.com/locate/jss

Cross-layer end-to-end label switching protocol for WiMAX–MPLS heterogeneous networks[☆]

Jenhui Chen[a,*], Woei-Hwa Tarn[a], Wu-Hsiao Hsu[b], Chih-Chieh Wang[a]

[a] Department of Computer Science and Information Engineering, Chang Gung University, 259 Wen-Hwa 1st Road, Kweishan, Taoyuan 333, Taiwan, ROC
[b] Department of Computer Science and Information Engineering, Ming Chuan University, Kweishan, Taoyuan 333, Taiwan, ROC

ARTICLE INFO

Article history:
Received 18 July 2011
Received in revised form 9 May 2012
Accepted 9 May 2012
Available online 6 June 2012

Keywords:
Cross-layer
Label switching
MPLS
Network
Protocol
WiMAX

ABSTRACT

The integration of WiMAX networks and multi-protocol label switching (MPLS) networks, called WiMPLS networks, is the trend for nomadic Internet access in the fourth generation (4G) wireless networks. The base station (BS) in such heterogeneous networks will play the role of bridge and router between the IEEE 802.16 subscriber stations (SSs) and MPLS networks. However, there is no such integrated solution so far and the switching efficiency of the BS should be considered as well. This paper, therefore, adopts a cross-layer fashion (from network layer to MAC layer) to design the *end-to-end label switching protocol* (ELSP) for filling this gap. ELSP provides the mechanism of end-to-end (SS-to-SS) and layer 2 switching transfer for switching performance enhancement by assigning the SS with the MPLS labels (M-labels). The M-label can be carried by the IEEE 802.16e extended subheader within the MAC protocol data unit (MPDU), which is fully compliant with the IEEE 802.16e standard. The security issue caused by M-label usage is also concerned and solved in this paper. This paper also reveals an extra advantage that the switching delay of the BS achieved by ELSP can be as low as hardware-accelerated IP lookup mechanism, e.g., ternary content addressable memory (TCAM). Simulation results show that ELSP efficiently improves the end-to-end transfer delay as well as the throughput for WiMPLS heterogeneous networks.

1. Introduction

The multi-protocol label switching (MPLS) technology is investigated for supporting service differentiation and traffic engineering in backbone networks (Le Faucheur, 1998; Nagarajan and Ekici, 2008). In recent years, there is a great demand for extending the capability of MPLS to wireless access networks for mobile access support (Langar et al., 2006, 2009). Meanwhile, an emerging broadband wireless access technology, the IEEE 802.16d/e standard (IEEE Working Group, 2004, 2006), is proposed for nomadic users in metropolitan area networks (MAN), also known as WiMAX (worldwide inter-operability for microwave access) networks. Nevertheless, the standard does not provide the mechanism of how to integrate WiMAX and MPLS networks.

In WiMAX networks, the base station (BS) plays the role of router/gateway to route packets from subscriber stations (SSs) to wired networks or vice versa (Chen et al., 2005). Consequently, the BS needs to play the role of bridge to convert packets from WiMAX networks to MPLS networks. Although Chen and Wang (2009) proposed a cross-layer cut-through switching mechanism (CCSM) for shortening the processing delay, this mechanism can only be applied in WiMAX local area networks (LANs) but cannot be extended to MPLS networks because MPLS uses the label switched path (LSP) label to route packets (Le Faucheur, 1998; Metz, 2001). Thus how to integrate WiMAX and MPLS networks (WiMPLS networks for short) efficiently, which motivates this work, is still an open issue (Dai and Chiang, 2007; Le Faucheur et al., 2002).

Several research works (Langar et al., 2006, 2009) focus on feasible frameworks to enhance the performance of the layer 2 transmission in the MPLS-wireless networks. Langar et al. (2006) present the mechanism of *micro mobile MPLS*, which integrates the mobile IP and MPLS protocols by using two-level hierarchy architecture. However, such a scheme cannot avoid IP lookup in the BS. Langar et al. (2009) show an *adaptive Master Residing Area* (MRA) which alleviates the limitations of previous works and benefits from MPLS resource provisioning capability, which can manage adaptively the mobile node according to its current state and the quality-of-service (QoS) constraints. Similarly, none of them contribute to the integration of WiMAX and MPLS networks.

In the IEEE 802.16e protocol (IEEE Working Group, 2004, 2006), the data packets from SS are packed or fragmented into one or several MAC protocol data units (MPDUs) before their transmission. It

☆ This work was supported in part by the National Science Council, Taiwan, ROC, under Contract NSC100-2221-E-182-030.
* Corresponding author. Tel.: +886 3 211 8800x5990; fax: +886 3 211 8700.
E-mail address: jhchen@mail.cgu.edu.tw (J. Chen).

0164-1212/$ – see front matter © 2012 Elsevier Inc. All rights reserved.
http://dx.doi.org/10.1016/j.jss.2012.05.050

uses the transport connection identifier (TCID) number instead of IP address for MPDU transmission. The transferred MPDUs, which arrive in the BS, will be unpacked or defragmented into data packets for further IP lookup process. After the termination of IP lookup process of each data packet, the data packet will be fragmented or packed again into MPLS data units before entering the MPLS networks. The succession of packet conversion will lead to an inevitable delay in the WiMPLS networks.

The IEEE 802.16e standard provides an extended subheader (ES) function for carrying additional or extended information for particular operations. The motivation of this paper is that if the MPLS label (M-label) can be known by the SS, the SS can use the ES function to carry the M-label and then let the BS switch data frames in the MAC layer to MPLS backbone for *end-to-end transmission* in WiMPLS networks. In this way, the SS will share some loading of BS for routing packets and the BS only has to extract the M-label from the ES field and then forward it to the next M-label switching router (LSR) without much delay. To enable this, we began to investigate an SS initiated and cross layer enabled (from the network layer, L3, to the MAC layer, L2) end-to-end label switching protocol (ELSP) to let the BS have the capability for supporting the end-to-end packet transmission. Fig. 1 shows the general concept of the ELSP implementation as compared with the legacy way of WiMAX and MPLS integration. Notice that the BS plays the gateway of the first mile or the last mile when the both terminals are WiMAX users. In this way, packets can be fast transferred from one terminal to another terminal over these two types of networks. It is especially suitable for the multimedia streaming applications, e.g., the mobile voice over IP (VoIP) or mobile video conference, etc.

To evaluate the performance of ELSP, this paper gives a series of simulation and tests by comparing ELSP with two representative state-of-the-art IP lookup mechanisms, the software–hardware integrated solution called *fast IP lookup (FIPL)* (Taylor et al., 2003) and the hardware-depended special memory chip solution called *ternary content addressable memory (TCAM)* (Zheng et al., 2006). The results show ELSP can achieve as low switching delay as TCAM-enabled switch. This is another advantage of ELSP when integrating two types of networks. The main contribution of ELSP are highlighted below.

- ELSP provides a cross-layer, end-to-end (SS-to-SS) label-switching mechanism for packet forwarding in WiMPLS networks. The SSs can be either remote SSs or local SSs.
- The IP lookup will be taken only once by the BS when the SS does not have the M-label to its destination IP mapping notified by its serving BS (SBS). This advantage will be more significant especially in multimedia flows, which have the same source to destination pair.
- The packet forwarding delay is approximate to the IP lookup delay achieved by the hardware accelerated mechanism, e.g., TCAM. In other words, ELSP does not need expensive memory chips to achieve high performance.
- ELSP is fully compatible with the IEEE 802.16e protocol.
- ELSP provides the local SS-to-SS L2 switching mechanism within a BS's service area.

The remainder of this paper is organized as follows. Section 2 demonstrates details of ELSP mechanism and the intranet SS-to-SS switching mechanism. Section 3 presents the ELSP system model and corresponding delay and throughput estimation. The numerical analysis of the performance evaluation is given in Section 4. Section 5 presents the simulation results of the proposed mechanism. Finally, the conclusion and the future works are discussed in Section 6.

2. End-to-end label switching protocol (ELSP)

To enable the packet transmission through two different types of MAC configurations, which avoids the network IP lookup process, a MAC layer assisted switch routing has to be implemented in the intermediate node between these two configurations. The BS plays the role of intermediate node, which connects the wireless part and the wired part and, therefore, transfers the IEEE 802.16 data frames to the MPLS data frames. The IEEE 802.16e protocol provides a subheader extension scheme for further protocol extension usages.

First, on the side of the IEEE 802.16 protocol, the data frame is conveyed with the TCID as the identifier. Contrarily, on the side of the LSP, the data frame is conveyed and switched with the

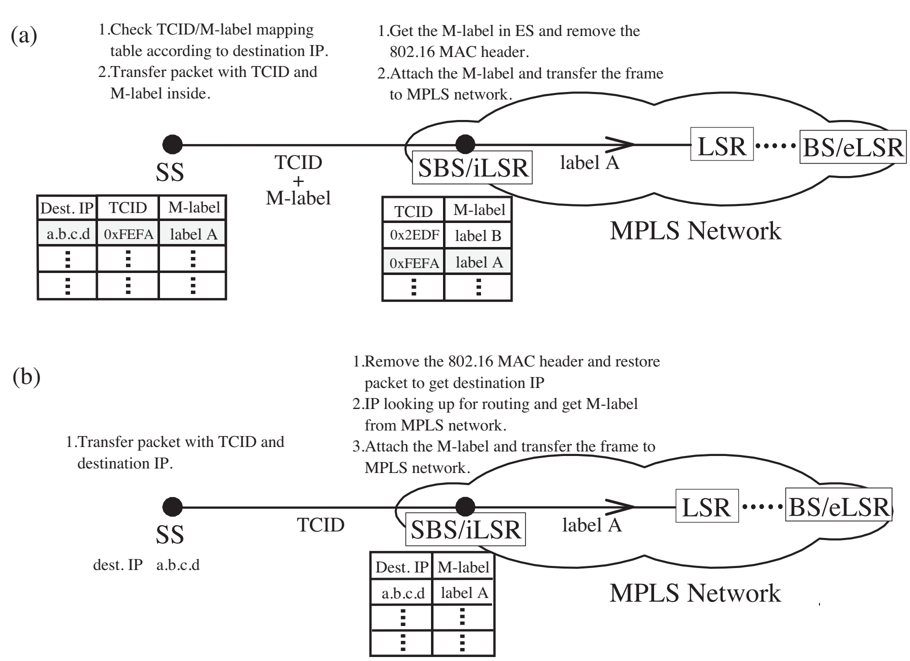

Fig. 1. The diagram of packet switching between ELSP and MPLS networks: (a) the ELSP mechanism and (b) the legacy way.

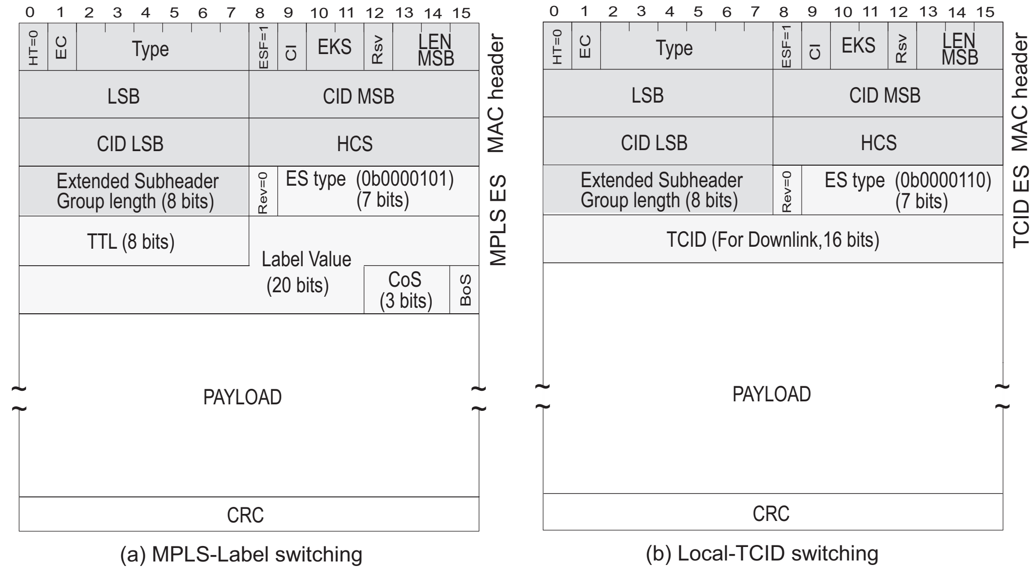

Fig. 2. The standard IEEE 802.16e data frame header format with subheader extension: (a) the new subheader extension of M-label with ES type coded as 0b0000101 and (b) the new subheader extension of local TCID number with ES type coded as 0b0000110.

M-label (Langar et al., 2008). Therefore, the BS has to be capable of identifying the coming data frames as the outgoing traffic[1] or the local (turnaround) traffic.[2] The ELSP uses the ES of the MAC header function (IEEE Working Group, 2006), i.e., two reserved ES types, for SSs to indicate the transferred data frame belonging to the outgoing traffic or the local traffic. Fig. 2 shows two different header formats of the proposed ES formats in details. The extended subheader appears if the ES field (ESF), which is the ninth bit of the MAC header, is set as one. Otherwise, the ES is absent.

The packet transmission from SSs to the BS can be classified as three categories: (1) the packets are targeted to an Internet node which does not belong to the IEEE 802.16 serving area, (2) the packets are targeted to an Internet node which belongs to the IEEE 802.16 serving area, and (3) the local traffic. Since the first two kinds are outgoing traffic, they will be treated as the same procedure. Therefore, in this paper, ELSP will focus on two kinds of traffic categories. The first one is the end-to-end label switching transfers from one WiMAX network to another WiMAX network through MPLS networks and the second one is the local traffic WiMAX switching. These two categories are separately discussed in the following subsections.

2.1. The outgoing traffic

If an SS has packets to send to Internet, it will first send a bandwidth request (BR) frame with a TCID to the BS for acquiring the required bandwidth for sending data. At this stage, the SS has to wait until the BS responds. After receiving the BR frame from the SS, the BS has to forward the bandwidth request to the connection admission control (CAC) process to determine to accept the request or not. If the request finally is accepted, the BS will issue a bandwidth grant frame back to the SS. After receiving the bandwidth grant frame, the SS sends MAC protocol data units (MPDUs) to the BS with the TCID. Once the BS receives MPDUs from the SS, it will determine whether these MPDUs are local traffic or outgoing traffic. To enable this, the BS has to assemble these MPDUs into an original data packet and then forward it to the network layer for IP lookup process. Taking Fig. 3 as a reference, ELSP takes the procedure as shown below when an SS has a packet to transmit to Internet.

Step 1: SS_A uses the associated TCID to transmit MPDUs to its SBS, which plays the role of ingress LSR (iLSR) or called the *edge LSR* (ELSR) of MPLS networks. A complete IP packet including the IP header and its payload is enclosed in the MPDU.

Step 2: After receiving the MPDUs, the SBS/iLSR takes the unpacking/defragmenting process of MPDUs and forwards the IP packet to the network layer for IP lookup process.

Step 3: The SBS/iLSR performs the label distribution protocol (LDP) and the MPLS network creates the label switching table in each LSR along the route.

Step 4: The SBS/iLSR replies the correlated label back to SS_A for following packets delivery, which target to the same destination IP address. The BS creates an TCID to M-label entry in the mapping table for label switching usage and possible security usage.[3]

Step 5: If the targeted destination (SS_B) belongs to another IEEE 802.16 BS's serving area, the remote BS (treated as an egress LSR, eLSR) will set up a TCID for downlink usage and create the MPLS-to-TCID mapping table for end-to-end transmission.

Step 6: After the M-label notification, SS_A starts to transmit MPDUs and enables the MPLS ES by setting the ESF=1. The ES type for MPLS usage is coded as 0b0000101 as shown in Fig. 2(a). The M-label notified by the SBS/iLSR is filled in the label value field of the MPLS ES for fast layer 2 switching.

Step 7: The SBS/iLSR receives MPDUs from SS_A and transforms IEEE 802.16 MPDUs into MPLS packets, and then forwards MPLS packets through the MPLS route.

Step 8: Finally, BS/eLSR receives MPLS packets with the M-label and transforms MPLS packets into IEEE 802.16 MPDUs according to the established MPLS-to-TCID mapping table, and then directly transmits MPDUs to SS_B.

[1] The traffic where SSs communicate with the service area out of the BS, e.g., Internet.

[2] The intranet traffic where SSs communicate with each other within the service area of one BS.

[3] We will introduce and present the security part of ELSP in Section 2.3 later.

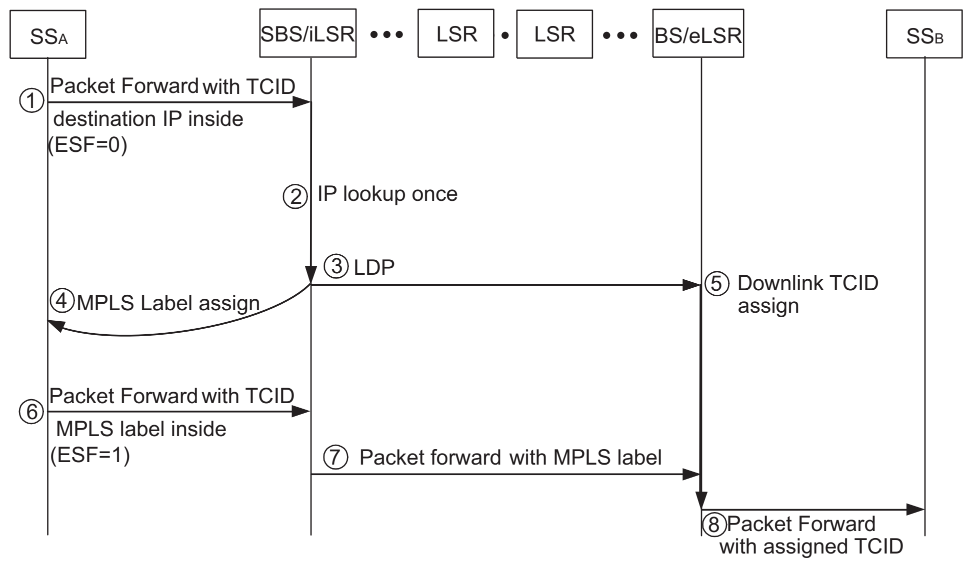

Fig. 3. The transmission identification process of outgoing traffic in the ELSP.

Above described steps show the flow of an SS making the connection from end-to-end layer 2 label switching mechanism over WiMPLS networks. The process of M-label obtainment is required when an SS does not have the IP to M-label mapping record. The SBS/iLSR shall maintain a TCID-to-M-label table for security checking and management among SSs. Once the SS has the entry for the destination associated with specific service type, the SS can send data packets with their corresponding TCIDs for QoS transmissions.

2.2. The local traffic

In order to shorten the process of each end-to-end packets transmission inside the serving area of a BS, ELSP applies a fast cross-layer switching concept (Chen and Wang, 2009) to reduce the local packets transmission delay. This mechanism is achieved by letting SS transmit MPDUs with the assigned TCID and associated with the next hop destination's TCID transmitted by the BS in the downlink. Notice that each SS shall maintain an IP to TCID mapping table for data transmission. Each time the SS changes its destination IP address, the SS should ask the BS for IP lookup process to renew the IP to TCID mapping. The making and reservation procedures are shown in Fig. 4 and its corresponding algorithm.

Step 1: SS_A uses the assigned TCID associated with one of QoS service types to transmit packets to its SBS. A complete IP packet including the IP header and its payload is encapsulated in the MPDU.

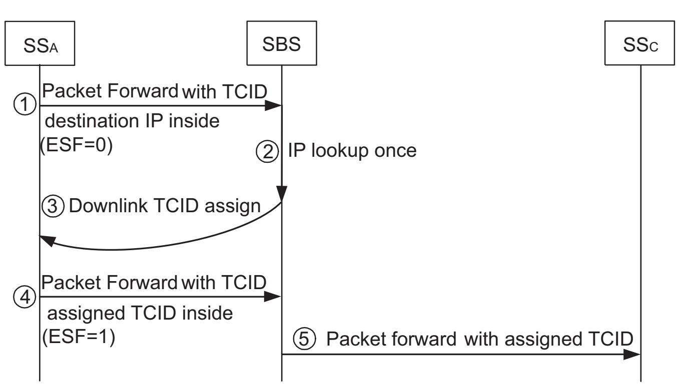

Fig. 4. The transmission identification process of local traffic in the ELSP.

Step 2: After receiving the MPDUs, the SBS unpacks/defragments the MPDU and forwards these packets to the network layer for IP lookup process. After the IP lookup process, the SBS assigns a TCID for downlink transmission of these packets.

Step 3: The SBS then forwards another TCID (downlink) number to SS_A for upcoming packet delivery.

Step 4: SS_A transmits MPDUs with the TCID (uplink) and attaches the related TCID (downlink) to the ES by setting ESF = 1. The ES type for the local traffic usage is coded as 0b0000110 as shown in Fig. 2(b).

Step 5: The SBS forwards MPDUs transmitted from SS_A with the indicated TCID associated within the MPDUs to SS_C directly without involving the L3 IP lookup process.

2.3. The security issue

As we introduced in the prior sections, the use of M-label is carried in the ES field of the MAC header of transferred MPDUs. To prevent the problem of avoiding an SS using M-labels it should not use, the M-label notification (from the SBS to the SSs) and M-label security checking should be introduced in the BS. Firstly, the transmission of M-label notification by the SBS uses the wired equivalent privacy (WEP) security protocol to prevent the M-label from being stolen by malicious SSs. Secondly, since the transfer of ES field of the MAC header is not encrypted, it may be overhearing easily by malicious SSs. To prevent malicious SSs from using M-labels which are gotten by overhearing the ES of legal transmissions, the SBS can apply the checking process of TCID to M-label mapping. If the TCID to M-label is consistent, the frames will be forwarded. Otherwise, these frames will be dropped immediately. Notice that TCID is identical and cannot to be used by other SSs because any attempt on using other SSs' TCIDs to transmit frames will cause collisions.

Furthermore, if an SS attempts to use a fake TCID and a fake M-label to upload frames in its uplink transmission burst, which is allowed by the SBS with a different TCID number, the transmitted frames will be blocked by the SBS because the TCID of the transmitted frames does not match the allowed TCID of transmission. Besides, TCID to M-label checking process will not cause a lot of overhead since TCID is the index of the TCID-to-M-label checking table.

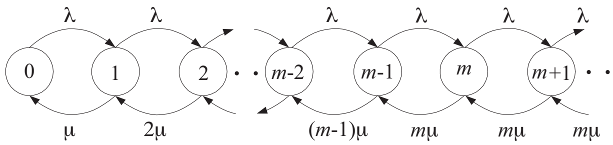

Fig. 5. The rate transition diagram for the $M/M/m$ queue.

3. System model

In this section, we introduce a system model to evaluate the ELSP performance in the aspect of the system processing delay and the throughput, respectively. This model bases on the Markov chain $M/M/m$ queueing model and focuses on the uplink transfer delay and the throughput of outgoing traffic in the BS. Assume SSs connect to a centralized BS over wireless fading channels, where multiple connections (data flows) are supported by the BS. Each SS can make multiple connections to the BS simultaneously based on its bandwidth requests.

The uplink resource allocation process is treated as a multi-server $M/M/m$ model as shown in Fig. 5. Assume the arrival rate λ (the average number of requests per frame) follows Poisson distribution. There are m servers, and each of them has an independently and identically distributed exponential service time distribution with mean $1/\mu$ (the average needed number of frames a request requires for service). The required bandwidth of each request per frame from SSs follows the exponential distribution with a mean length $N_s = k/\mu$ (slots). We notice that each request means a same source-to-destination (end-to-end) flow transmission. This implies that a request will comprise several packets targets to the same destination. Let C denote the capacity of the resource of uplink (the number of slots per frame). Based on the CAC rules, each request is allowed to have the resource of mean k slots per frame for transmission if it is given permission to enter the system. The model satisfies the condition $C \geq mk$. We let $r = \lambda/\mu$ be the offered work load rate and $\rho = r/m = \lambda/m\mu$ be the offered work load rate to a server.

According to the $M/M/m$ model, we utilize the birth–death processes (Gross et al., 2008) with steady-state probabilities to get the expected queue size L_q in the MAC as

$$L_q = \left(\frac{r^m \rho}{m!(1-\rho)^2}\right) p_0, \tag{1}$$

where p_0 represents the probability of zero number of the SS accessing the system and is equal to $1/[(r^m/m!(1-\rho) + \sum_{n=0}^{m-1} r^n/n!]$, where $\rho < 1$. To find the expected steady-state MAC access waiting time T_M, we use the queueing delay T_q and the Little's formulas (Beutler, 1983), $L = \lambda T$ and $L_q = \lambda T_q$, where L and L_q represent the numbers of requests in the MAC and queues, respectively; to get $T_M = 1/\mu + T_q = 1/\mu + L_q/\lambda$ and we have

$$T_M = \frac{1}{\mu} + \frac{r^m}{m!(m\mu)(1-\rho)^2}\left(\frac{r^m}{m!(1-\rho)} + \sum_{n=0}^{m-1}\frac{r^n}{n!}\right)^{-1}. \tag{2}$$

In the following, we discuss three different kinds of IP lookup mechanisms, the software IP lookup mechanism, the hardware accelerated IP lookup mechanism, and ELSP approach for performance analysis, respectively.

3.1. The delay of software–hardware IP lookup

The IP lookup process in the BS can be modeled as an $M/M/1$ model, since the output of an $M/M/m$ queue is identical to its input (Burke, 1956). Assume the length of each packet in the request is an exponential distribution with a mean length ℓ in slots. Let $h = k/\ell\,\mu$ be the number of packets in a request, the mean number of packets arrival rate from MAC layer to the IP lookup will be $\lambda_p = \lambda h = \lambda k/\ell\,\mu$. Therefore, the packet arrival rate to the IP lookup will be $\lambda' = \lambda_p + \lambda_I$, where λ_I is the mean packet arrival rate from Internet. Let μ_S denote the mean service rate of the software–hardware IP lookup process (the number of packets per frame). Thus $\rho' = \lambda'/\mu_S$ is the work load rate to the IP lookup server queue and the software–hardware IP lookup processing delay will be

$$t_S = \frac{L'}{\lambda'} = \frac{\rho'}{\lambda'(1-\rho')} = \frac{1}{\mu_S - \lambda'}, \tag{3}$$

where $L' = \rho'/(1-\rho')$.

Assume the M-label lookup process takes delay t_m. The software–hardware system processing delay T_S in the BS can be obtained from

$$\begin{aligned} T_S &= t_m + t_S + T_M \\ &= t_m + \frac{\mu + \mu_S - \lambda'}{\mu\mu_S - \mu\lambda'} + \frac{r^m/(m!(m\mu)(1-\rho)^2)}{((r^m/(m!(1-\rho))) + (\sum_{n=0}^{m-1}(r^n/n!)))}. \end{aligned} \tag{4}$$

3.2. The delay of hardware IP lookup

The hardware accelerated IP lookup processing delay T_H is similar with T_S but has different value of the IP lookup delay. Let μ_H be the hardware IP lookup processing rate, then the IP lookup processing delay will be $t_H = 1/(\mu_H - \lambda')$. According to Eq. (4), we have

$$\begin{aligned} T_H &= t_m + t_H + T_M \\ &= t_m + \frac{\mu + \mu_H - \lambda'}{\mu\mu_H - \mu\lambda'} + \frac{r^m/(m!(m\mu)(1-\rho)^2)}{((r^m/(m!(1-\rho))) + (\sum_{n=0}^{m-1}(r^n/n!)))} \end{aligned} \tag{5}$$

3.3. The delay of ELSP

In ELSP, the IP lookup process will be taken only once if the source–destination IP pair is same. We notice that each request comprises of several packets to the same destination. Moreover, since the ELSP maintains an M-label to TCID mapping table in the BS, the incoming Internet traffic will not take the IP lookup process (an end-to-end fast layer 2 label to TCID switching). Thus, the input traffic to the network layer for IP lookup is identical to λ. Then, the offered work load to IP lookup is $\rho_E = \lambda/\mu_E$ and the IP lookup processing delay would be

$$t_E = \frac{L_E}{\lambda} = \frac{\rho_E}{\lambda(1-\rho_E)} = \frac{1}{\mu_E - \lambda}, \tag{6}$$

where μ_E is the ELSP's IP lookup processing rate and $L_E = \rho_E/(1-\rho_E)$.

Because the M-label notification process only proceeds once for the same destination IP address, the t_n is ignored here. Since the TCID-to-M-label security checking process has to be taken in the BS, the security checking processing time t_c should be considered here. Thus, the system processing delay of ELSP in the BS T_E is given as

$$\begin{aligned} T_E &= t_c + t_E + T_M \\ &= t_c + \frac{\mu + \mu_E - \lambda}{\mu\mu_E - \lambda\mu} + \frac{r^m/(m!(m\mu)(1-\rho)^2)}{((r^m/(m!(1-\rho))) + (\sum_{n=0}^{m-1}(r^n/n!)))}. \end{aligned} \tag{7}$$

Table 1
Modulation parameter (IEEE Working Group, 2006).

Modulation/coding rate	Data rate (bits/slot)
QPSK 1/2	144
16-QAM 1/2	288
64-QAM 3/4	648

3.4. Throughput

The system throughput we measure here focuses on the IP lookup throughput of the uplink data transmission including different modulation and coding schemes. The uplink IP lookup output rate of ELSP, the software–hardware integrated mechanism, and hardware accelerated mechanism are $1/T_E$, $1/T_S$, and $1/T_H$, respectively. The uplink throughput of ELSP S_E can be calculated as

$$S_E = \frac{\lambda k}{\ell \mu}\frac{1}{T_E}\ell N_b N_f = \frac{\lambda k}{\mu T_E}N_b N_f, \tag{8}$$

where N_f is the number of frames per second and N_b is the number of bits per slot. The parameter N_b varies with different modulation and coding schemes and is equal to $3N_d r_m r_c$, where N_d represents the number of data subcarriers per slot, r_m is the number of bits per subcarrier to which modulation applies, e.g., the 16-QAM for 4 bits/subcarrier and r_c is the coding rate, e.g., 1/2 or 2/3, respectively. Similarly, the throughput of software–hardware integrated mechanism S_S and hardware accelerated mechanism S_H will be

$$S_S = \frac{\lambda k}{\mu T_S}N_b N_f \tag{9}$$

and

$$S_H = \frac{\lambda k}{\mu T_H}N_b N_f, \tag{10}$$

respectively.

4. Numerical results

This section illustrates the effects of average processing delay, required bandwidth, number of servers, and throughput under different μ, N_s, m, and N_b with different mechanisms. T_S, T_E, T_H, S_S, S_E, and S_H are the measuring parameters. In the following analysis, we adopt FIPL (Taylor et al., 2003) as the software IP lookup processing mechanism to get the delay T_S obtained from Eq. (4) and TCAM (Zheng et al., 2006) as the hardware IP lookup processing mechanism to get the delay T_H obtained from Eq. (5). The IP lookup process speed of FIPL is 1 MHz (one million lookups per second) (Taylor et al., 2003) or μ_S = 5000 lookups/frame (1 μs per lookup). The speed of TCAM IP lookup process is 133 MHz (Zheng et al., 2006) or μ_H =66,666 lookups/frame (75 ns per lookup).

According to the IEEE 802.16 standard, there are 35 subchannels in one channel in the uplink and each of them has 24 orthogonal frequency-division multiple access (OFDMA) data symbols. Considering the steady-state condition $\rho < 1$, the mean requests arrival rate per frame is $\lambda = \rho m \mu$, $\rho < 1$. The capacity of one slot depends on different modulation and coding schemes as shown in Table 1. Assume, in the uplink portion of each frame, two subchannels are reserved for initial ranging and bandwidth contention usage and the allowed bandwidth for each request is $k = 24$ slots per frame (based on QoS policy). Thus only 264 slots are available for data transmission and the maximum number of servers in the system (channels) is $m = 264/k = 11$ when $k = 24$.

Assume the ratio of the packet arrivals of the Internet to the intra-net is 8 : 2. Thus, according to Eq. (3), the packet arrival rate to the IP lookup process $\lambda' = \lambda_p + \lambda_I = 5\lambda_p$ or $\lambda' = 5\lambda k/\ell\,\mu$ since $\lambda_p = \lambda k/\ell\,\mu$. The length of each frame is 5 ms long and the ratio of downlink to uplink is 2:1. In the numerical analysis, only the uplink transmission is studied. The M-label lookup process delay t_m in the iLSR is equal to 1 μs (Chang et al., 2000). For the packet length, we use the workload statistical analysis in 2008 provided by The Cooperative Association for Internet Data Analysis (CAIDA) for IPv4 and IPv6 data packets (CAIDA, 2008). It shows the statistical length of Internet packets cover about 50% of 50 bytes ($\ell \approx$ 1.4 slots), 20% of 750 bytes ($\ell \approx$ 20.8 slots), and 30% of 1500 bytes ($\ell \approx$ 41.6 slots). Therefore, we set the mean packet length as 625 bytes ($\ell \approx$ 17.3 slots) in our numerical analysis. The related mean request length N_s, allowed bandwidth per frame k by QoS policy, and corresponding service rate μ are listed in Table 2.

Table 2
Analysis parameters.

Parameter	Value		
Request length (bytes)	625	1250	2500
No. of slots N_s	18	36	72
μ (m = 11, k = 24)	24/18	24/36	24/72
μ (m = 22, k = 12)	12/18	12/36	12/72
μ (m = 44, k = 6)	6/18	6/36	6/72

4.1. The effect of processing delay

First, the average system processing delay from the time the packet requests to access the media to the time it finishes the M-label switching in the BS is studied. Three mechanisms ELSP, FIPL, and TCAM are compared in T_E, T_S, and T_H. We set the mean packet length ℓ as 18 slots and the uplink modulation and coding rate is 16-QAM 1/2. Fig. 6 shows the results obtained from Eqs. (4), (5) and (7), respectively. We can see from the results that the three lines intertwine together since the average $T_M \gg t_E, t_S$, and t_H. That means the IP lookup processing delay is much smaller than the MAC access waiting time. As we can see in Fig. 6, the software solution ELSP can achieve as low delay as hardware accelerated solution TCAM and can outperform software–hardware integrated solution FIPL about 1000 ns.

On the other hand, comparing T_E with T_H, ELSP can achieve a lower IP lookup processing delay of 25 ns in average than that of 75 ns achieved by TCAM. It is important that ELSP can achieve high performance as expensive hardware does by using the software way. In other words, ELSP can use a smart protocol to avoid unnecessary IP lookup and save the time to transmit more packets,

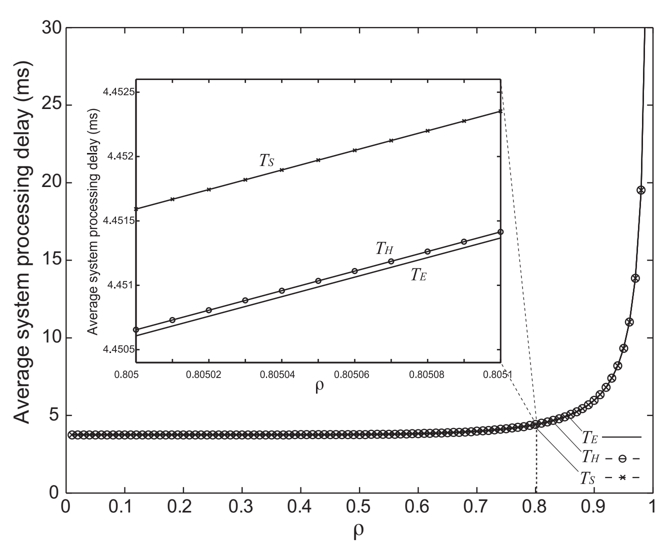

Fig. 6. Average processing delay vs. work load ρ when m = 11, k = 24, ℓ=18, and μ = 1.33 with the transmission rate 16-QAM 1/2.

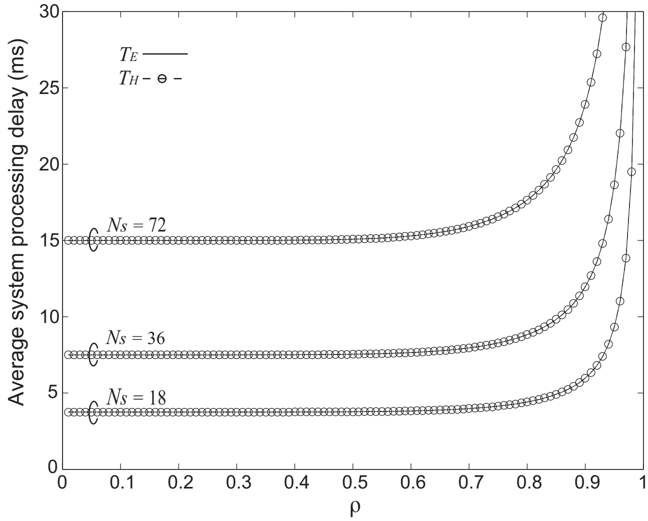

Fig. 7. Average processing delay vs. work load ρ under different request lengths N_s = 18, 36, or 72 slots/frame and μ = 24/18, 24/36, or 24/72 when k = 24 and m = 11.

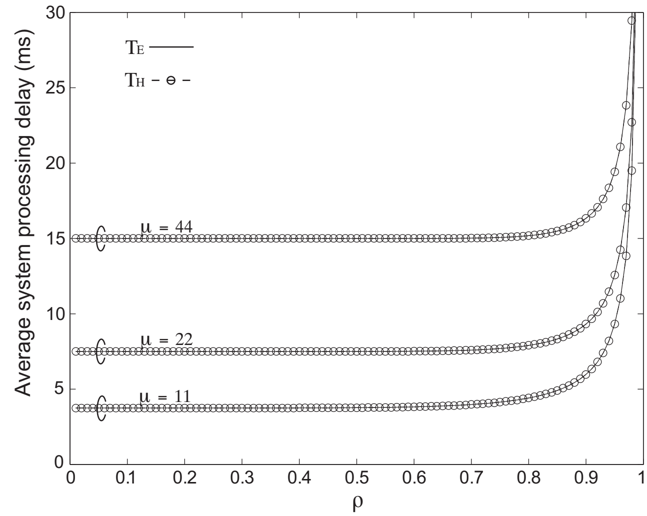

Fig. 8. Average processing delay vs. work load ρ under different m = 11, 22, or 44 and μ = 24/18, 12/18, or 6/18 when N_s = 18.

and thus achieve the similar delay effect as good as the hardware mechanism.

4.2. The effect of required bandwidth from SSs

The average system processing delay is evaluated by using different number of slots per request N_s. The hardware mechanism TCAM and ELSP are compared in this subsection. Fig. 7 illustrates the influence of different value of N_s = 18, 36, and 72 slots on T_H and T_E. The average system processing delay is obtained by increasing the work load ρ under the 16-QAM 1/2 modulation and coding scheme. In Fig. 7, both T_H and T_E increase with increasing ρ. There is no doubt that when ρ is high, congestion could happen in both two mechanisms. T_H and T_E have approximate value in the system processing delay, however, T_E still has lower value than T_H in each case. This means that ELSP can achieve as low delay as TCAM in whatever size of request. We also observe that the average system delay increases by increasing the length of request. It is obvious that the processing delay will be prolonged if the size is increased. It is notable that ELSP can keep a stable system processing delay until $\rho \approx 0.95$. This is because ELSP uses a smart mechanism to enable the router to identify only the first packet of a flow and assigns the M-label to let the SS carry this information to bypass the IP lookup process. ELSP is especially useful for the end-to-end flow-based multimedia communications in WiMPLS networks because the IP lookup processing delay is significant reduced.

4.3. The effect of number of servers

The allowed number of concurrent connections of data transmissions determined by the CAC mechanism will influence the performance of the transmission system. It is interesting to observe the system processing delay when the maximal allowed number of connections (servers) varies. The number of servers m is set to 11, 22, or 44 and μ = 24/18, 24/36, or 24/72 when N_s = 18. Fig. 8 shows that the system processing delay increases with increasing m in both TCAM and ELSP. It shows that the allowable number of connections will affect the average packet access delay. The delay will increase when the number of allowed connections by CAC increases. This is because that the allocated bandwidth for each connection per frame will decrease when the number of connections increases.

4.4. The effect of throughput

The system throughput S is taken into consideration in different modulation schemes in this subsection. Fig. 9 shows the throughput of TCAM S_H and ELSP S_E in KB/s by using different modulation and coding schemes QPSK 1/2, 16-QAM 1/2, and 64-QAM 3/4, respectively. The carried bits per slot is shown in Table 1. The S is evaluated by increasing ρ to validate the correctness of Eqs. (8) and (10) when m = 11, k = 24, N_S = 18, and μ = 24/18. As shown in the figure, the maximum throughput of ELSP and TCAM with 64-QAM 3/4, 16-QAM 1/2, or QPSK 1/2 reaches 865 KB/s, 1730 KB/s, or 3892 KB/s when ρ reaches 0.79. The throughput we investigate here is the system throughput. That is, the throughput is measured in the total bandwidth output per second that packets go through from the SS to the end of packets switched out by M-label in the SBS (the iLSR). Therefore, the exact throughput is less than the uplink bandwidth by using corresponding modulation and coding scheme in the uplink due to the longer delay of T_M.

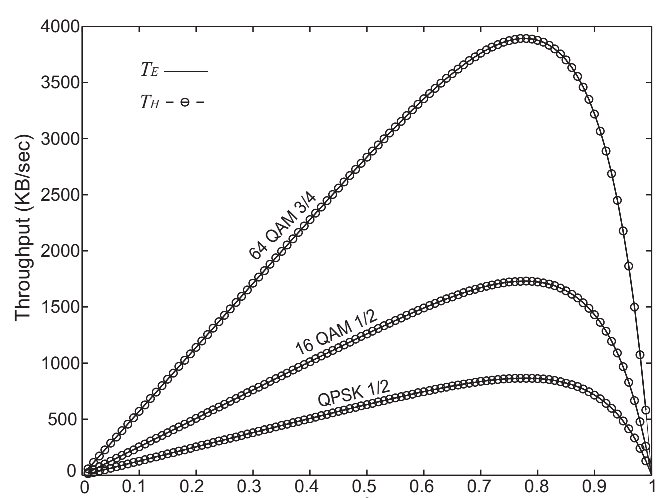

Fig. 9. The uplink throughput vs. work load ρ when m = 11, k = 24, N_s = 18, and μ = 24/18.

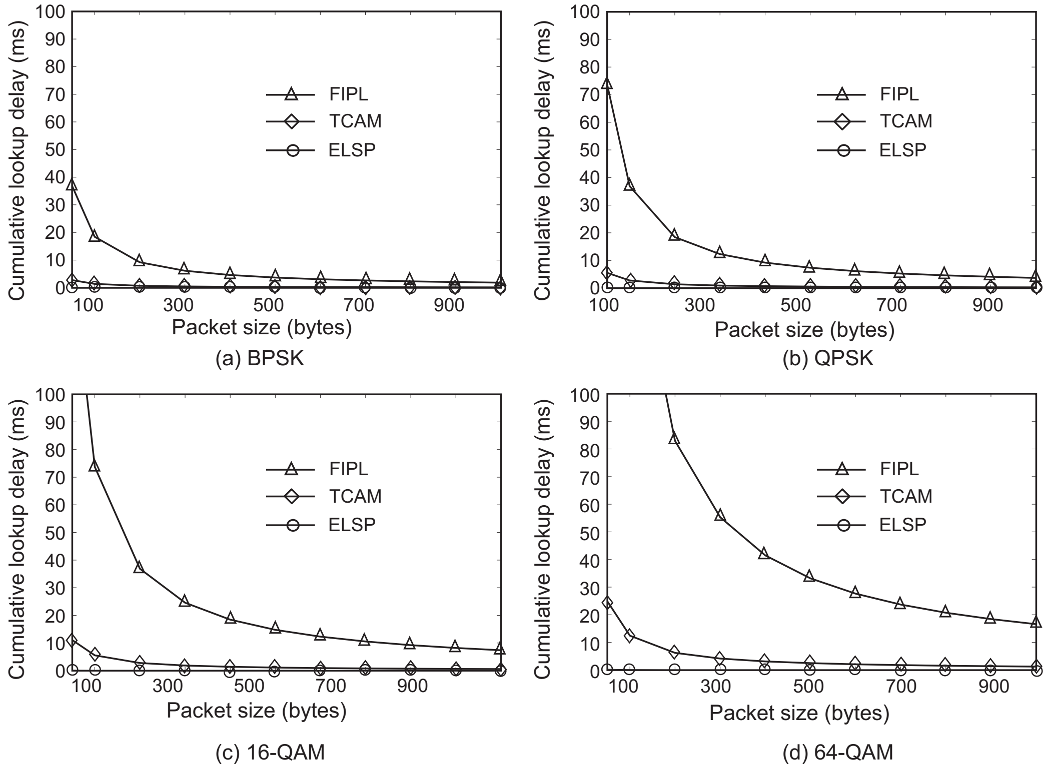

Fig. 10. The comparisons of the cumulative IP lookup delay vs. the packet size by different modulation schemes.

4.5. The worst case of IP lookup

This subsection discusses the IP lookup processing delay in the worst case as the routing/forwarding engine processes shortest packets at maximum rate under the saturated condition. The cumulative delay is to gather the statistics of IP lookup processing time in the SBS persisting for 1 s. Fig. 10 shows the impact of different sizes of forwarded packets on the IP lookup delay among FIPL, TCAM, and ELSP. As we can see from Fig. 10 that ELSP can obtain a relatively lower lookup delay in all modulation schemes. It is obvious that, under the saturated condition, the number of packets for IP lookup is getting larger when the size of packet becomes small. A larger number of packets for IP lookup processing will lead to a heavy IP lookup load and, thus, gets a longer IP lookup delay. However, we can see that ELSP always outperforms the other two approaches because ELSP's IP lookup process is reduced due to the cross-layer label switching mechanism.

5. Simulation results

To evaluate the performance of ELSP mechanism above, the QualNet simulation tool (http://www.scalable-networks.com/support/documentation/#qualnet_5.0) is adopted in the simulation. The simulation scenario is configured as four SSs (the end users) equally divided by two groups distributed in the two ends of WiMPLS networks, i.e., $m = 11$, as shown in Fig. 11. Two BSs play the role of wireless access point for the SSs and the MPLS ELSRs concurrently by adopting the ELSP mechanism. Three LSRs are located between these two BSs and provide the MPLS switching capability. The bandwidth of MPLS links is 10 Mbits/s. The propagation delay between two LSRs is 1 μs and the MPLS switching time takes 1 μs.

Table 3
The IEEE 802.16e system parameters.

Parameter	Volume
OFDMA frame length	5 m
Bandwidth	20 MHz
downlink/uplink ratio	1:1
DCD/UCD period	5 s
No. of OFDMA symbol per frame	49
No. of uplink subchannels	70
OFDMA symbol time	100.84 μs
FFT size (N_{FFT})	2048
Sampling frequency (F_s)	22.86 MHz

The simulation environment is set as a 1500 m × 1500 m square. The line-of-sight (LOS) distance between two BSs is set 1500 m but the real distance of the routing path for packet switching is longer than LOS distance as shown in Fig. 11. All simulation parameters of the WiMAX BS follows the specification of the IEEE 802.16e standard (IEEE Working Group, 2006) as described in Table 3.

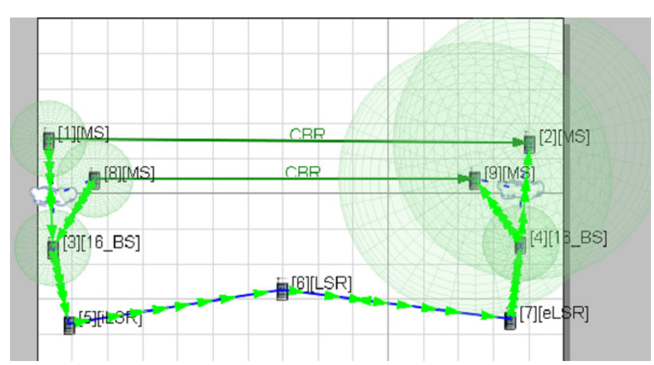

Fig. 11. A snapshot of the simulation topology.

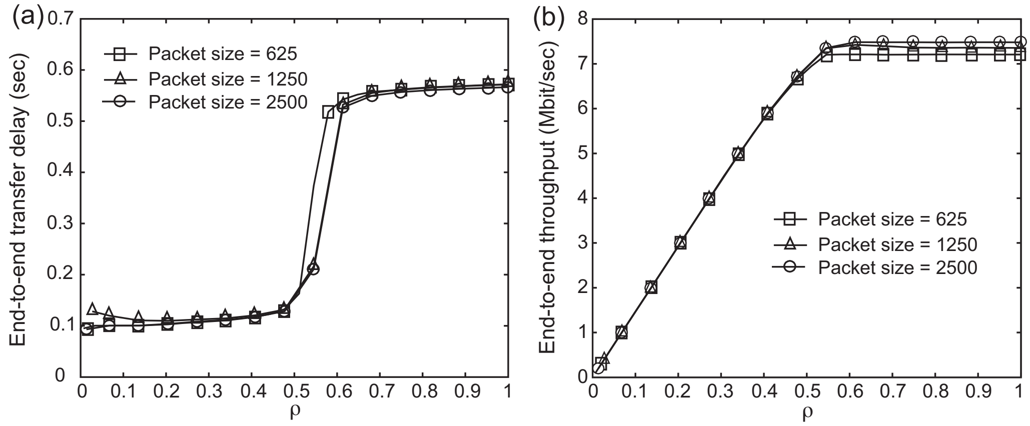

Fig. 12. The comparisons of the end-to-end transfer delay and throughput in terms of one SS to one SS transmission over WiMPLS networks when $m = 11$, $k = 24$, and $\mu = 24/18$.

The wireless medium is operated in TDD mode and each OFDMA frame length is 5 ms long and the ratio of downlink to uplink is 1:1. The two generated traffics considered in the simulation are both the one way input, that is, the traffics first generated in the left-hand side two SSs, see Fig. 11, and go through the WiMPLS networks and finally downloaded to the right-hand side SSs, respectively.

The simulation run time lasts 100 s (20,000 frames) to collect wanted system performance results, e.g., the end-to-end transfer delay and throughput. There are two BSs connected with MPLS networks and each of them serves several SSs, respectively. The type of service flows is considered as the non-real-time polling service (nrtPS), which is generated from the application tool set. To increase the representativeness, the different packet sizes, i.e., 625 bytes/packet, 1250 bytes/packet, and 2500 bytes/packet, are introduced in the scenario. The traffic load is started from 0.1 to 1, which is aimed to the uplink capacity of the BS and varies following the increment of packet arrival rate λ to each SS. That is, the simulation results will show the performance measurement in aspect of end-to-end transfer delay and throughput to investigate the performance of ELSP.

Figs. 12 and 13 show the end-to-end transfer delay and throughput in terms of a single flow or multiple flows over the WiMPLS networks. Both simulation results show that the end-to-end transfer delay increases following the increment of the traffic load ρ. The results consist with the analytical results that the delay sustains in a lower delay time and then rises up sharply when ρ approaches the point of system saturated condition. The reason why the rising point of the end-to-end transfer delay approximate $\rho = 0.5$ of Fig. 12(a) and $\rho = 0.2$ of Fig. 13(a) are earlier than the point of analytical result ($\approx$0.8) is that the simulated transfer delay is the end-to-end delay measurement. This result explains two phenomena. First, the end-to-end transfer delay is affected by the number of LSRs. Secondly, the increment of the number of SSs will lead to a longer average end-to-end transfer delay as shown in Figs. 12(a) and 13(a). This result shows that the increment of the number of SSs will cause the contention and thus influence the delay time. We will note that the end-to-end transfer delay finally sustains in a stable value when $\rho > 0.6$ in Fig. 12(a) and $\rho > 0.3$ in Fig. 13(a). This is because, in the QualNet simulator, the delay calculation will only count the packets outputted to the final destination. Therefore, the end-to-end transfer delay will finally reach a stable value. Moreover, the impact of different mean packet lengths on the end-to-end transfer delay is minor as shown in Figs. 12(a) and 13(a).

Figs. 12(b) and 13(b) show the throughput of the one pair of transmission scenario and two pairs of transmission scenario under different average packet sizes. As we can see from the results, the value of maximum throughput decreases when the number of SSs increases. The throughput will reach the statured condition when $\rho = 5.4$ in Fig. 12(b) and $\rho = 2.7$ in Fig. 13(b). It is obvious that the con-

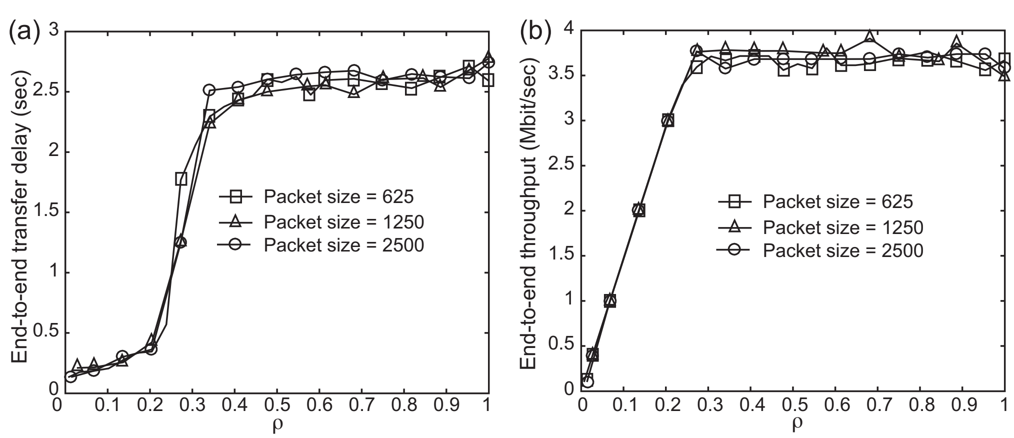

Fig. 13. The comparisons of the end-to-end transfer delay and throughput in terms of two SSs to two SSs transmission over WiMPLS networks when $m = 11$, $k = 24$, and $\mu = 24/18$.

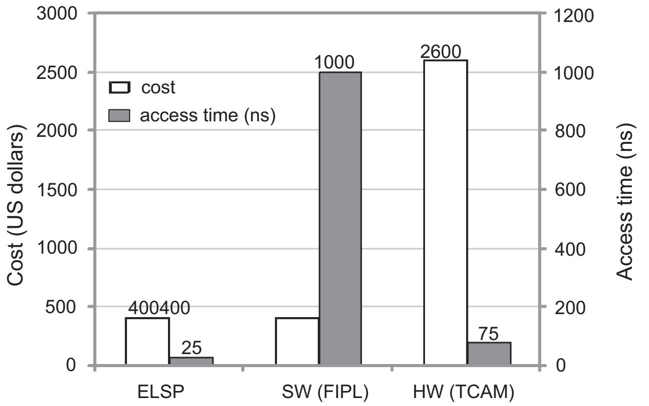

Fig. 14. Cost vs. access time at three mechanisms.

tention between two SSs and the lower priority of the nrtPS service will lead to a longer delay and thus induces the lower throughput.

Finally, Fig. 14 compares the cost versus the access time among ELSP, FIPL, and TCAM, respectively. The data shows that TCAM can achieve a 75 ns access time in average but costs as six times as the cost of FIPL and ELSP. However, on the other hand, ELSP can achieve an average 25 ns access time[4] but does not need to spend much cost. In other words, ELSP uses the software solution to obtain a lower packet switching delay same as the achievement of hardware-enabled approach but costs very little as compared with the hardware-enabled approach, i.e., the cost of ELSP is about two-thirteenth of TCAM. This result shows that ELSP is a good solution for fast packet switching without involving the network layer by only using the software approach and can achieve as high performance as the hardware-enabled scheme.

6. Conclusions

In this paper, we investigated a solution of integrating WiMAX networks and MPLS backbone networks. The proposed ELSP uses the software methodology to assist the BS to be able to (1) switch local and remote streaming data in the L2, (2) play the role of ELSR to the MPLS networks, and (3) provide the end-to-end L2 label switching between two SSs. The performance measurement of ELSP in terms of the system access delay of the BS, the throughput of the BS, the end-to-end transfer delay, the end-to-end throughput, and the cost of implementation shows that ELSP gets outstanding representation as compared with TCAM and FIPL. The characteristic of end-to-end L2 transmission of ELSP is suitable for more and more multimedia streaming applications nowadays. The security of ELSP, which avoid unwanted SSs using other SSs' M-labels to transfer data, is also considered and presented in this paper. The success of ELSP encourages us to apply multimedia applications over the heterogeneous networks (wire and wireless).

Finally, the size of IP to TCID and M-label lookup table has to be investigated further in order to keep the freshness of the table and limit the growth of the table. One way to keep the size of the mapping table growing within a boundary, the freshness of each record in the table can associate with a timer. The investigation of how long this time will be is an interesting research topic further in order to avoid the performance degradation of ELSP.

[4] The achieved average access time depends on the length of the streaming data comes from the application layer. In other words, the bigger the streaming data size is the lower the average access time will be.

References

Beutler, F., 1983. Mean Sojourn times in Markov queueing networks: Little's formula revisited. IEICE Transactions on Information Theory 29 (May (2)), 233–241.

Burke, P.J., 1956. The output of A queueing system. Operations Research 4, 699–714.

CAIDA, 2008. Packet Size Distribution Comparison between Internet Links in 1998 and 2008, Available: http://www.caida.org/research/traffic-analysis/pkt_size_distribution/graphs.xml.

Chang, G.K., et al., 2000. A proof-of-concept, ultra-low latency optical label switching testbed demonstration for next generation internet networks. In: Proc. Optical Fiber Communication 2000, vol. 2, Baltimore, MD, March 2000, pp. 56–58.

Chen, J., Wang, C.-C., 2009. Cross-layer cut-through switching mechanism for IEEE 802.16d/e wireless networks. IEEE Communications Letters 13 (October (10)), 779–781.

Chen, J., Pang, A.-C., Sheu, S.-T., Tseng, H.-W., 2005. High performance wireless switch protocol for IEEE 802.11 wireless networks. Mobile Networks and Applications 10 (October (5)), 741–751.

Dai, J.-W., Chiang, L.-F., 2007. Hierarchical wireless mobile MPLS mechanism using foreign tracking agent based on M/G/1 with capacity C queueing model. IET Communications 1 (October (5)), 903–908.

Gross, D., Shortle, J.F., Thompson, J.M., Harris, C.M., 2008. Fundamentals of Queueing Theory, 4th ed. Wiley, Hoboken, NJ.

IEEE 802.16 Working Group, 2004. IEEE Standard for Local and Metropolitan Area Networks-Part 16: Air Interface for Fixed Broadband Wireless Access Systems, IEEE Std. 802. 16-2004, October 2004.

IEEE 802.16 Working Group, 2006. IEEE Standard for Local and Metropolitan Area Networks-Part 16: Air Interface for Fixed and Mobile Broadband Wireless Access Systems. IEEE Std. 802. 16e-2005, February 2006.

Langar, R., Tohme, S., Bouabdallah, N., 2006. Mobility management support and performance analysis for wireless MPLS networks. ACM Wiley International Journal of Network Management 16 (July (4)), 279–294.

Langar, R., Bouabdallah, N., Boutaba, R., Aug. 2008. A comprehensive analysis of mobility management in MPLS-based wireless access networks. IEEE/ACM Transactions on Networking 16 (4), 918–931.

Langar, R., Bouabdallah, N., Boutaba, R., Sericola, B., 2009. Proposal and analysis of adaptive mobility management in IP-based mobile networks. IEEE Transactions on Wireless Communication 8 (July (7)), 3608–3619.

Le Faucheur, F., 1998. IETF multiprotocol label switching (MPLS) architecture. In: Proc. ICATM-98, June 1998, pp. 6–15.

Le Faucheur, F., et al., 2002. Requirements for Support of DiffServ-Aware MPLS Traffic Engineering, IETF RFC 3270, May 2002.

Metz, C., 2001. Layer 2 over IP/MPLS. IEEE Internet Computing 5 (July–August (4)), 77–82.

Nagarajan, R., Ekici, E., Dec. 2008. An efficient and flexible MPLS signaling framework for mobile networks. Wireless Networks 14 (6), 859–875.

Taylor, D.E., Turner, J.S., Lockwood, J.W., Sproull, T.S., Parlour, D.B., 2003. Scalable IP lookup for internet routers. IEEE Journal of Selected Areas in Communications 21 (May (4)), 522–534.

Zheng, K., Hu, C., Lu, H., Liu, B., 2006. A TCAM-based distributed parallel IP lookup scheme and performance analysis. IEEE/ACM Transactions on Networking 14 (August (4)), 863–875.

Jenhui Chen received the B.S. and Ph.D. degrees in Computer Science and Information Engineering (CSIE) from Tamkang University, Taipei, Taiwan, R.O.C. in July 1998 and January 2003, respectively. Since 2003, he has been with the Department of CSIE, Chang Gung University, where he is currently an associate professor and a research fellow of the High Speed Intelligent Center (HSIC), Chang Gung University. His main research interests include design, analysis, and implementation of computer and communication networks, wireless networks, and network-on-chip (NoC) for system-on-chip (SoC) design.

Woei-Hwa Tarn was born in Taipei, Taiwan, R.O.C. He received his B.S. and M.S. degrees from Electrical and Electronic Engineering, Chung Cheng Institute of Technology, R.O.C. in 1978 and 1983, respectively. He is currently pursuing his Ph.D. degree at the Department of Electrical Engineering, Chang Gung University, Kweishan, Taoyuan, Taiwan, R.O.C. His main research interests include the 4G wireless network, power efficiency, and error control coding.

Wu-Hsiao Hsu received the Ph.D. degree in Department of Computer Science and Information Engineering from Tamkang University, Tamsui, Taipei, Taiwan in 1999. He is currently an associate professor in Department of Computer Science and Information Engineering at Ming Chuan University, Taoyuan Country, Taiwan. From 2000 to 2003, he served in the Eastern Multimedia Corporation (EMC) as a CTO and consultant, and was responsible for planning the ISP IP infrastructure and IDC operation. His recent research interests include QoS unicast/multicast routing, QoE, cloud computing and IPv6.

Chih-Chieh Wang received the B.S. degree in Electrical Engineering from Chinese Military Academy of R.O.C., in 1983, and his MBA in Information Management from National Defense Management College, Taipei, Taiwan, R.O.C. in 1999. He got his Ph.D. degree in Electrical Engineering from Chang Gung University, Taiwan, in 2010. His main research interests include analysis, and implementation of wireless network, MPLS network, and routing protocol.